

The Cairns-Tsallis model for ion acoustic cnoidal (periodic) waves

Forough Farhadkiyaei*

Abstract

In this paper, considering the importance of ion acoustic waves in nonlinear phenomena of plasma, the combined effects of nonextensivity and nonthermality parameters on the ion acoustic cnoidal nonlinear waves studied. In this regard, the hybrid Cairns-Tsallis distribution function used to describe the electrons and positrons. Conditions of formation of nonlinear ion acoustic waves and permissible values of nonextensivity (Q) and nonthermality (α) parameters were determined and the behavior of these waves with changes in these parameters in this type of plasma have been studied. For this purpose, we have used the reductive perturbation method (RPM) to derive the corresponding KdV equation for the ion acoustic wave, then considering the Sagdeev potential, the conditions for the generation of ion acoustic waves in the cnoidal and soliton form discussed. The effect of nonextensivity (Q) and nonthermality (α) parameters on the Sagdeev potential (potential well width and depth), wave amplitude and frequency investigated. The results show that for all of the acceptable values of Q and α the cnoidal ion acoustic wave is compressive.

Keywords

Electron-positron-ion plasma, Ion-acoustic nonlinear wave, Cnoidal wave, Sagdeev potential, The hybrid Cairns-Tsallis distribution.

Physics Department, Islamic Azad Uni., Aligudarz Branch, Aligudarz, Iran

*Corresponding author: foroughfarhadkiyaei@gmail.com

1. Introduction

Numerous observations clearly show the presence of energetic particles in plasma and astrophysical environments [1]. In space plasmas, there are coherent nonlinear waves and structures that play an important role [2], nonlinear phenomena and their properties in plasma depend mainly on plasma properties and particle distribution function. Observations from the Viking spacecraft [3] and the Freja satellite [4] show that there are electrostatic soliton structures in the magnetosphere that cannot expressed by the Maxwell distribution function. In this regard, Cairns et al. [5] proposed a nonthermal distribution function for plasma particles. This distribution function could express the presence of rarefactive ion acoustic solitary (IAS) structures very similar to what observed by the Viking spacecraft and the Freja satellite. In the nonthermal distribution function, the population of nonthermal particles is denoted by α , which varies between 0 and 1 ($0 < \alpha < 1$). In case $\alpha \rightarrow 0$, the Maxwell distribution function is retrieved. In this field, many researchers have assumed their research plasma model as a Cairns distribution function and have studied the phenomena in the presence of these particles. After Cairns, Tsallis generalized the Boltzmann-Gibbs entropy and proposed nonextensive statistical mechanics to describe systems that do not follow the Maxwell distribution function, such as systems with long-range interaction [6]. This distribution function is used commonly to describe various phenom-

ena in plasma, such as dissipative optical lattices [7], plasma wave propagation [7-9].

The main properties of the Tsallis distribution function are expressed by the parameter Q , which is called the degree of nonextensivity which in the case $Q < -1$, this distribution function is not normalized. The parameter Q in its normalized states has two separate states. one in part $-1 < Q < 1$ where the particles in this range cover all velocities and the other $Q > 1$ in which the distribution function has a cutoff on the maximum value. The permissible particle velocity is given by the following equation:

$$V_{max} = \left(\frac{2v_T}{Q-1} \right)^{\frac{1}{2}}, \quad v_T^2 = \frac{2KT}{m}$$

Here v_T is the thermal velocity of the plasma particles. T and m are the temperature and mass of the particles, respectively. A comparison of Maxwellian and nonextensive distribution function show, in the case $Q > 1$ high energy status are more likely in the Maxwellian distribution function .however, for $-1 < Q < 1$ high energy status are more probable in the nonextensive distribution function. In state $Q \rightarrow 1$, The Tsallis distribution function becomes the Maxwell-Boltzmann distribution functions.

In recent years, Tribche et al. [10] have studied ion acoustic solitary wave in a two-component electron-ion plasma with a nonextensive electron distribution. They concluded that this plasma model could explain both refractive and compressive

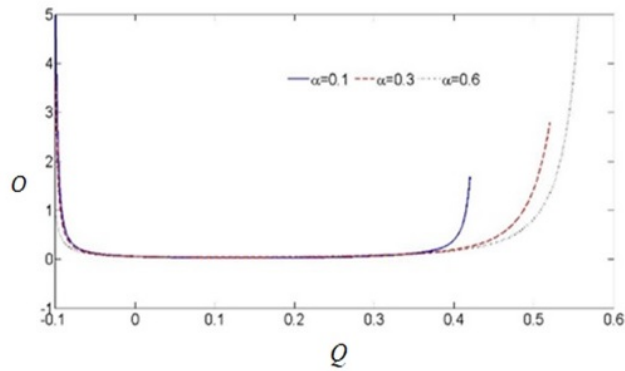


Figure 1. Plot of O versus Q for different α , having $\theta = 0.1$, $\vartheta = 0.1$, $V = 0.015$ and $\sigma_0 = -0.002$.

solitons, and these results led to the idea that nonthermal and nonextensive properties may be affect compressive or refractive in nature the ion’s soliton structures. As a result, Tribcheh et al. [11] generalized the Cairns model [5] and presented a hybrid Cairns–Tsallis velocity distribution that aims to increase the flexibility parameter in nonthermality plasmas. Such a two-parameter representation of the distribution function can be more consistent with observations of spatial plasmas [11]. Since Tribcheh et al. generalized the Cairns model and introduced the Cairns–Tsallis combination distribution function.

Many researchers used this distribution function in their research. For example, and Amour et al investigated the propagation of ion acoustic solitons in plasma with this distribution function that contains hot electrons [12]. In another study, Farooq et al used this hybrid distribution function in three-component plasma (e-p-i) to investigate the linear and nonlinear properties of ions paired with floating waves [13]. In a study, Bozit et al investigated the instability of ion acoustic waves in a non-collisional and nonmagnetic plasma, which included positive ions and electrons that followed this hybrid distribution function [14]. Benzka et al. and al-Taibani et al. Each separately investigated the properties of solitonic ion acoustic waves in the dust plasma, which has a combined distribution function of nonthermal and nonextensive [15, 16]. Williams et al studied the properties of the hybrid nonthermal nonextensive distribution function in the context of ion acoustic soliton behavior in plasmas with excess superthermal particles [17]. The head-on collisions of ion acoustic solitons and rogue waves in unmagnetized electronion plasma were carried out by El-Tantawy et al using the Cairns-Tsallis distribution for electrons [18]. Saha et al. [19] studied dust acoustic waves with ions featuring the Cairns-Tsallis distribution while Guo and Mei [20] presented the dust ion acoustic waves with electrons following the hybrid-distribution. Recently, several authors have adopted the Cairns-Tsallis distribution of particles to study the dynamics of electrostatic and electromagnetic waves in different plasma models [21–24].

In this paper, we investigate the combined effects of non-thermal and nonextensive parameters on the formation and

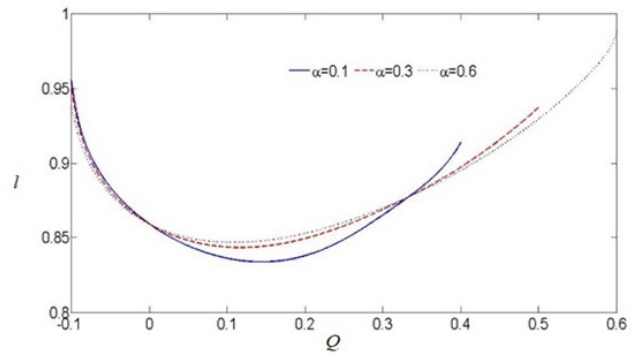


Figure 2. Plot of l versus Q for different α , having $\theta = 0.1$, $\vartheta = 0.1$, $V = 0.015$ and $\sigma_0 = -0.002$.

propagation of the ion acoustic cnoidal (periodic) wave in electron-positron-ion nonmagnetic plasma.

2. Basic equations

We consider a noncollisional and nonmagnetic plasma in this paper that includes a mixed fluid with Boltzmann positrons, nonthermal and nonextensive distributed electrons, and cold ions.

To model the effect of nonthermal and nonextensive electrons, we consider the following distribution function introduced by a number of researchers [11, 12].

$$f_e(v_x) = P_{Q,\alpha} \left(1 + \alpha \frac{v_x^4}{v_{te}^4} \right) \left[1 + (1 - Q) \frac{v_x^2}{2v_{te}^2} \right]^{\frac{1}{Q-1}} \quad (1)$$

In this distribution function, $v_{te} = \frac{T_e}{m}$ is the thermal velocity of the electron, T_e is the temperature of the electron, m_e is the mass of the electron, and $P_{Q,\alpha}$, is the constant of normalization which depends on Q and α , which is defined as follows.

$$P_{Q,\alpha} = N_{e0} \sqrt{\frac{m_e}{2\pi T_e}} \frac{\Gamma(\frac{1}{1-Q})(1-Q)^{\frac{5}{2}}}{\Gamma(\frac{1}{1-Q} - \frac{5}{2}) [3\alpha + (\frac{1}{1-Q} - \frac{3}{2})(\frac{1}{1-Q} - \frac{5}{2})(1-Q)^2]} \quad (2)$$

for, $-1 < Q < 1$

$$P_{Q,\alpha} = N_{e0} \sqrt{\frac{m_e}{2\pi T_e}} \frac{\Gamma(\frac{1}{Q-1} + \frac{3}{2})(Q-1)^{\frac{5}{2}} (\frac{1}{Q-1} + \frac{3}{2})(\frac{1}{Q-1} + \frac{5}{2})}{\Gamma(\frac{1}{Q-1} + 1) [3\alpha + (Q-1)^2 (\frac{1}{Q-1} + \frac{3}{2})(\frac{1}{Q-1} + \frac{5}{2})]} \quad (3)$$

for, $Q > 1$

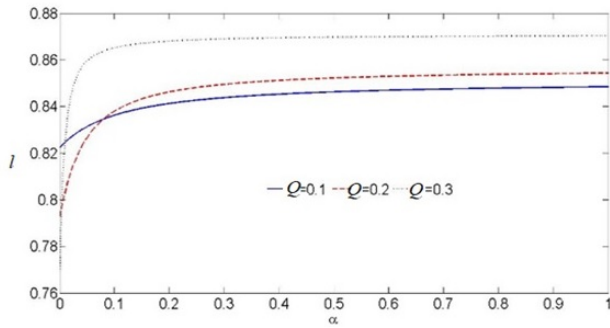


Figure 3. Plot of l versus α for different Q , having $\theta = 0.1$, $\vartheta = 0.1$, $V = 0.015$ and $\sigma_0 = -0.002$.

where parameter α determines the number of nonthermal electrons present in this plasma model. Γ is a Gamma function and Q is a parameter that measures the nonextensive properties of the system. By integrating equation 1 into the velocity space, the density of the number of electrons obtained as follows [11, 12].

$$N_e(\Phi) = \int_{-\infty}^{+\infty} f_e(v_e)dv \tag{4}$$

$$N_e(\Phi) = \int_{-v_{max}}^{+v_{max}} f_e(v_e)dv \tag{5}$$

$$N_e(\Phi) = N_{e0} \left[1 + \left(1 + (Q-1) \frac{e\Phi}{T_e} \right)^{\left(\frac{1}{Q-1} + \frac{1}{2} \right)} \right] \left[1 + A \left(\frac{e\Phi}{T_e} \right) + B \left(\frac{e\Phi}{T_e} \right)^2 \right] \tag{6}$$

$$A = \frac{-16Q\alpha}{3 - 14Q + 15Q^2 + 12\alpha} \tag{7}$$

$$B = \frac{16(2Q-1)Q\alpha}{3 - 14Q + 15Q^2 + 12\alpha} \tag{8}$$

In the nonextensive limit state ($Q \rightarrow 1$); the above density is converted to the following known nonthermal electron density [5].

$$N_e(\Phi) = N_{e0} \left[1 - \frac{4\alpha}{1 + 3\alpha} \left(\frac{e\Phi}{T_e} \right) + \frac{4\alpha}{1 + 3\alpha} \left(\frac{e\Phi}{T_e} \right)^2 \right] \exp \left(\frac{e\Phi}{T_e} \right) \tag{9}$$

In contrast, for $\alpha = 0$ the above density is converted to the electron density of the nonextensive which is as follows [6]. To model the effect of electron nonextensivity. The Q -distribution function or Tsallis distribution is considered as follows:

$$f_e(v_e) = P_Q \left[1 + (1-Q) \left(\frac{m_e v_e^2}{2T_e} - \frac{e\Phi}{T_e} \right) \right]^{\left(\frac{1}{Q-1} \right)} \tag{10}$$

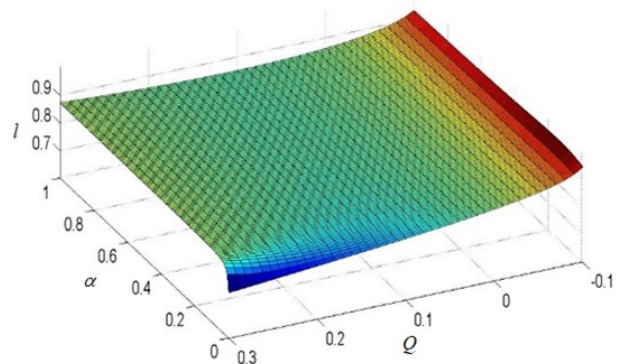


Figure 4. Plot of l versus α for different Q , having $\theta = 0.1$, $\vartheta = 0.1$, $V = 0.015$ and $\sigma_0 = -0.002$.

The constant of normalization P_Q is given by

$$P_Q = N_{e0} \sqrt{\frac{m_e(1-Q)}{2\pi T_e}} \frac{\Gamma\left(\frac{1}{1-Q}\right)}{\Gamma\left(\frac{1}{1-Q} - \frac{1}{2}\right)}, -1 < Q < 1 \tag{11}$$

$$P_{Q,\alpha} = N_{e0} \left(\frac{1+Q}{2} \right) \sqrt{\frac{m_e(Q-1)}{2\pi T_e}} \frac{\Gamma\left(\frac{1}{Q-1} + \frac{1}{2}\right)}{\Gamma\left(\frac{1}{Q-1}\right)}, Q > 1 \tag{12}$$

Here, the parameter Q defines for the strength of nonextensivity. It may be useful to note that for $Q < -1$, the Q -distribution is unnormalizable. In the extensive limiting case ($Q = 1$), the Q -distribution reduces to the well-known Maxwell-Boltzmann distribution. Note that for $Q > 1$, the Q -distribution function exhibits a thermal cutoff on the maximum value allowed for the velocity of the particles, which is given by

$$v_{max} = \sqrt{\frac{2T_e}{m_e} \left(\frac{e\Phi}{T_e} + \frac{1}{Q-1} \right)} \tag{13}$$

Integrating the Q -distribution over the velocity space, one obtains the following non-dimensional hot electron number

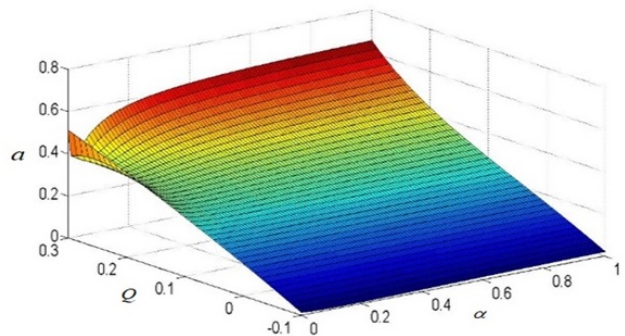


Figure 5. Plot of α versus α and Q , having $\theta = 0.1$, $\vartheta = 0.1$, $V = 0.015$ and $\sigma_0 = -0.002$.

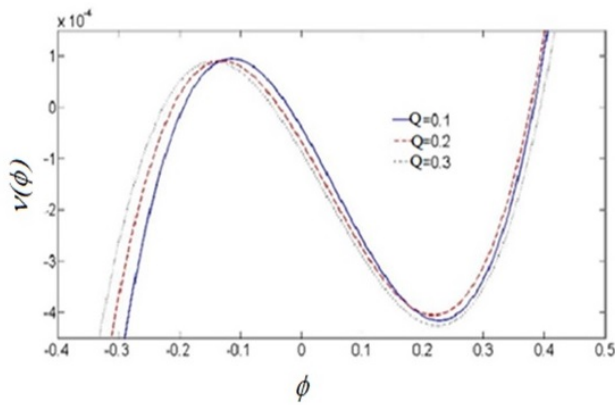


Figure 6. Plot of $v(\Phi)$ versus Φ for different Q , having $\theta = 0.1$, $\vartheta = 0.1$, $V = 0.015$ and $\sigma_0 = -0.002$.

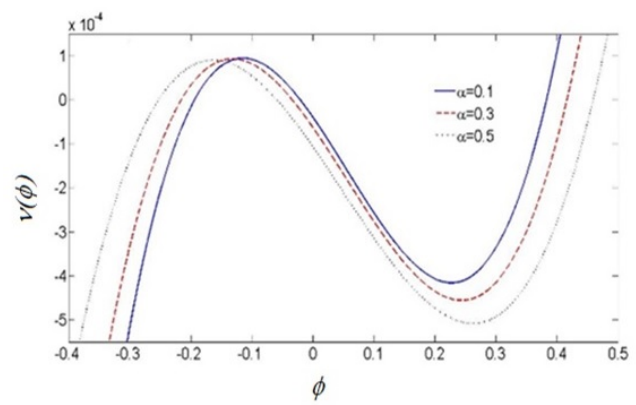


Figure 7. Plot of $v(\Phi)$ versus Φ for different α , having $\theta = 0.1$, $\vartheta = 0.1$, $V = 0.015$ and $\sigma_0 = -0.002$.

density [25, 26]

$$N_e(\Phi) = N_{e0} [1 + (1 + (Q - 1) \frac{e\Phi}{T_e})^{(\frac{1}{Q-1} + \frac{1}{2})}], Q > -1 \quad (14)$$

In addition, positrons with the Boltzmann distribution function are introduced as follows.

$$N_p(\Phi) = N_{p0} \exp[-\theta (\frac{e\Phi}{T_e})] \quad (15)$$

In the above equations Φ , N_e , N_p and N which are the electrostatic potential, the equilibrium densities of electrons, positrons and ions, respectively, and those with a zero index are equilibrium quantities. In addition, the propagation of ion acoustic waves along the x -axis assumed. Nonlinear behavior of ion acoustic waves by a set of normalized fluid equations described below.

$$\partial_t N + \partial_x (NU) = 0 \quad (16)$$

$$\partial_t U + U \partial_x U = -\partial_x \Psi \quad (17)$$

$$\partial_x^2 \Psi = N_e - pN_p - (1 - p)N \quad (18)$$

$$N_e = [1 + (Q - 1)\Psi]^{(\frac{1}{Q-1} + \frac{1}{2})} \times [1 + A\Psi + B\Psi^2] \quad (19)$$

$$A = \frac{-16Q\alpha}{3 - 14Q + 15Q^2 + 12\alpha} \quad (20)$$

$$B = \frac{16(2Q - 1)Q\alpha}{3 - 14Q + 15Q^2 + 12\alpha} \quad (21)$$

$$N_p = \exp(-\theta\Psi) \quad (22)$$

For small Ψ , it is expanded as follows:

$$N_p = 1 - \theta\Psi + \frac{\theta^2\Psi^2}{2} + \dots \quad (23)$$

$$N_e = 1 + M_1\Psi + M_2\Psi^2 + \dots \quad (24)$$

$$M_1 = A + (\frac{Q+1}{2}) \quad (25)$$

$$M_2 = B + (\frac{Q+1}{2})A + (\frac{(Q+1)(3-Q)}{8}) \quad (26)$$

where $\vartheta = N_{p0}/N_{e0}$, $\theta = T_e/T_p$, $\Psi = e\Phi/T_e$ and ϑ is the ratio of positrons to electrons in equilibrium. In the above equations, the velocity u , the potential Φ , the time t , and the spatial coordinates x are normalized by the speed of the ion acoustic wave C_s , the thermal potential T_e/e the inverse of the characteristic plasma frequency ω_{pi}^{-1} , and the Debye length $\lambda_D = (\frac{\epsilon_0 T_e}{N_0 e^2})^{\frac{1}{2}}$. The ion density N , the electron density N_e , and the positron density N_p are normalized to their corresponding equilibrium densities, respectively. T_p and T_e are the temperatures of the positron and electron fluxes, respectively. In this case, it is assumed that the destruction time of the positrons is longer than the inverse frequency characteristic of the ion acoustic wave. Under such conditions, it can be assumed that the destruction of the positron by the electron is negligible and the destruction of the positrons can be neglected.

3. Derivation of KdV equation and solutions of KdV equation

To obtain the KdV equation from the basic equations 16 to 22, we introduce the following extended coordinates

$$\zeta = \zeta^{\frac{1}{2}}(x - v_0 t) \quad (27)$$

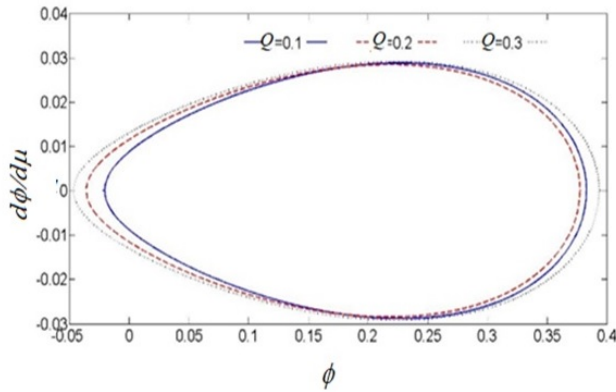


Figure 8. Plot of $d\Phi/d\mu$ versus Φ for different Q , having $\theta = 0.1$, $\vartheta = 0.1$, $V = 0.015$ and $\sigma_0 = -0.002$.

$$\tau = \zeta^{\frac{3}{2}} t \tag{28}$$

where ζ is a small parameter that determines the intensity of the nonlinearity, and v_0 is the phase velocity of the wave. Dependent variables are expanded as follows.

$$N = 1 + \zeta N_1 + \zeta^2 N_2 + \zeta^3 N_3 + \dots \tag{29}$$

$$U = \zeta U_1 + \zeta^2 U_2 + \zeta^3 U_3 + \dots \tag{30}$$

$$\Psi = \zeta \Psi_1 + \zeta^2 \Psi_2 + \zeta^3 \Psi_3 + \dots \tag{31}$$

By substituting the expressions 29 to 31 within Eqs. 16 to 18 and by using Eqs. 23 and 28, expressions with the lowest order ζ obtained.

$$-v_0 \partial_\zeta N_1 + \partial_\zeta U_1 = 0 \tag{32}$$

$$-v_0 \partial_\zeta U_1 + \partial_\zeta \Psi_1 = 0 \tag{33}$$

$$\Psi_1 (M_1 + \vartheta \theta) - (1 - \vartheta) N_1 = 0 \tag{34}$$

By integrating Eqs. 32 and 33 with respect to ζ for a continuous wave that can have even limited perturbation at $\zeta \rightarrow \pm\infty$. We have the following relation between the first-order disturbed quantities.

$$N_1 = \left(\frac{M_1 + \vartheta \theta}{1 - \vartheta} \right) \Psi_1 \tag{35}$$

$$U_1 = v_0 \left(\frac{M_1 + \vartheta \theta}{1 - \vartheta} \right) \Psi_1 + C_1(\tau) \tag{36}$$

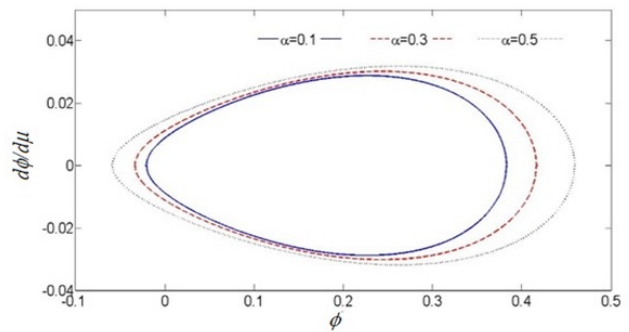


Figure 9. Plot of $d\Phi/d\mu$ versus Φ for different α , having $\theta = 0.1$, $\vartheta = 0.1$, $V = 0.015$ and $\sigma_0 = -0.002$.

C_1 is an integration constant that is independent of ζ what may be dependent on the variable τ . From these two Eqs. 35 and 36, the phase velocity of ion acoustic waves can be obtained as follows.

$$v_0 = \left(\frac{M_1 + \vartheta \theta}{1 - \vartheta} \right)^{-\frac{1}{2}} \tag{37}$$

Higher order equations considered as follows.

$$-v_0 \partial_\zeta N_2 + \partial_\tau N_1 + \partial_\zeta U_2 + \partial_\zeta (N_1 U_1) = 0 \tag{38}$$

$$-v_0 \partial_\zeta U_2 + \partial_\tau U_1 + U_1 \partial_\zeta U_1 + \partial_\zeta \Psi_2 = 0 \tag{39}$$

$$\partial_\zeta^2 \Psi_1 = (M_1 + \vartheta \theta) \Psi_2 + \left(M_2 - \frac{\vartheta \theta^2}{2} \right) \Psi_1^2 - (1 - \vartheta) N_2 \tag{40}$$

By Multiplying v_0 on both sides of Equation 38 and its difference from Equation 39 and using the first-order solutions, we obtain the following relation.

$$\partial_\zeta U_2 = \frac{v_0}{2} \partial_\zeta N_2 + \frac{1}{2v_0} \partial_\zeta \Psi_2 - \frac{1}{2v_0^3} \Psi_1 \partial_\zeta \Psi_1 + \frac{1}{2v_0} \partial_\tau C_1 \tag{41}$$

From equation 40, we have N_2 as follows.

$$N_2 = \left(\frac{M_1 + \vartheta \theta}{1 - \vartheta} \right) \Psi_2 + \frac{M_2 - \frac{\vartheta \theta^2}{2}}{1 - \vartheta} \Psi_1^2 - \frac{1}{1 - \vartheta} \partial_\zeta^2 \Psi_1 \tag{42}$$

Substitute N_2 obtained from the above equation into Equation 41, resulting in the following equation.

$$\begin{aligned} \partial_\zeta U_2 = & \frac{1}{v_0} \partial_\zeta \Psi_2 + \frac{1}{v_0} \left(\frac{M_2 - \frac{\vartheta \theta^2}{2}}{M_1 + \vartheta \theta} - \frac{1}{v_0^2} \right) \partial_\zeta (\Psi_1^2) \\ & - \frac{1}{2v_0(M_1 + \vartheta \theta)} \partial_\zeta^3 \Psi_1 + \frac{1}{2v_0} \partial_\tau C_1 \end{aligned} \tag{43}$$

By integrating this equation with respect to ζ , we have:

$$U_2 = \frac{\Psi_2}{v_0} + \left(\frac{M_2 - \frac{\vartheta \theta^2}{2}}{M_1 + \vartheta \theta} - \frac{1}{v_0^2} \right) \frac{\Psi_1^2}{v_0}$$

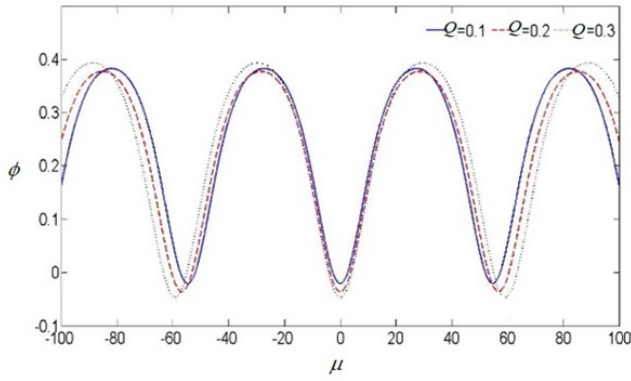


Figure 10. Plot of the electrostatic potential Φ versus μ for different Q , having $\theta = 0.1$, $\vartheta = 0.1$, $V = 0.015$ and $\sigma_0 = -0.002$.

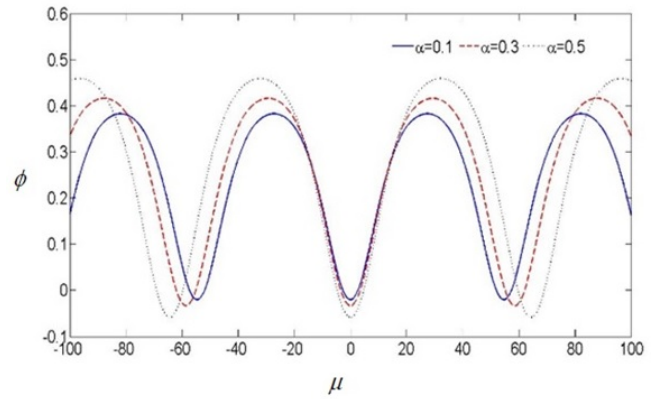


Figure 11. Plot of the electrostatic potential Φ versus μ for different α , having $\theta = 0.1$, $\vartheta = 0.1$, $V = 0.015$ and $\sigma_0 = -0.002$.

$$-\frac{1}{2\nu_0(M_1 + \vartheta\theta)} \partial_{\zeta}^2 \Psi_1 + C_2(\tau) \tag{44}$$

In the above equation, $C_2(\tau)$ which is the second integration constant, is independent of ζ but may be dependent on τ . Derived from Equation 44, periodic boundary conditions imply that:

$$\partial_{\tau} C_1 = 0 \tag{45}$$

Therefore C_1 is independent of ζ and τ . Now, to prove the KdV equation, we substitute the expression $\partial_{\zeta} U_2$ of equation 39 into equation 38 and use the first-order solutions, equations 35 and 36. We will have the following relationships.

$$\begin{aligned} \partial_{\zeta} N_2 &= \frac{2}{\nu_0^3} \partial_{\tau} \Psi_1 + \frac{3}{V_0^4} \Psi_1 \partial_{\zeta} \Psi_1 \\ &+ \frac{2}{\nu_0^3} C_1 \partial_{\zeta} \Psi_1 + \frac{1}{\nu_0^2} \partial_{\zeta} \Psi_2 + \frac{1}{\nu_0^2} \partial_{\tau} C_1 \end{aligned} \tag{46}$$

By differentiating Eq 40 with respect to ζ and substituting $\partial_{\zeta} N_2$ for equation 46, we have

$$\partial_{\tau} \Psi_1 + a \Psi_1 \partial_{\zeta} \Psi_1 + C_1 \partial_{\zeta} \Psi_1 + b \partial_{\zeta}^3 \Psi_1 = 0 \tag{47}$$

This equation is the required KdV equation that describes the evolution of the first order-perturbed potential (Ψ_1) the coefficients a and b are given below.

$$a = \frac{3}{2\nu_0} - \nu_0 \frac{M - 2\frac{\vartheta\theta^2}{2}}{M_1 + \vartheta\theta} \tag{48}$$

$$b = \frac{\nu_0^3}{2(1 - \vartheta)} \tag{49}$$

a and b are the nonlinear coefficient and the dispersion coefficient of the KdV equation, respectively. It is clear that the

nonlinear and dispersion coefficients depend on the temperature rate of the electron to positron θ , the relative density of the positron to the electron ϑ , the strength of nonextensivity Q , and the population of nonthermal particles α . In the extensive limiting state ($Q \rightarrow 1$), the above coefficients are converted to the following nonthermal state, which was previously reported in an article by Alinejad [27].

$$a = \frac{3}{2\nu_0} - \nu_0 \frac{1 - \vartheta\theta^2}{1 - \frac{4\alpha}{1+3\alpha} + \vartheta\theta} \tag{50}$$

$$b = \frac{\nu_0^3}{2(1 - \vartheta)} \tag{51}$$

$$\nu_0 = \sqrt{\frac{1 - \vartheta}{1 - \frac{4\alpha}{1+3\alpha} + \vartheta\theta}} \tag{52}$$

In the nonextensivity limiting case ($\alpha \rightarrow 0$), the nonlinear and dispersion coefficients will be as follows, which were previously studied by Dorrnian et al [28].

$$a = \frac{3}{2\nu_0} - \nu_0 \frac{(\frac{3-Q}{4}(Q+1) - \vartheta\theta^2)}{2(\frac{Q+1}{2} + \vartheta\theta)} \tag{53}$$

$$b = \frac{\nu_0^3}{2(1 - \vartheta)} \tag{54}$$

The phase velocity in this case is:

$$v = \sqrt{\frac{1 - \vartheta}{\frac{Q+1}{2} + \vartheta\theta}} \tag{55}$$

In order to find the steady state cnoidal and solitary wave solutions of the KdV Eq 47. We follow the same procedure as already done in Kaladze et al. [29, 30], and we have used

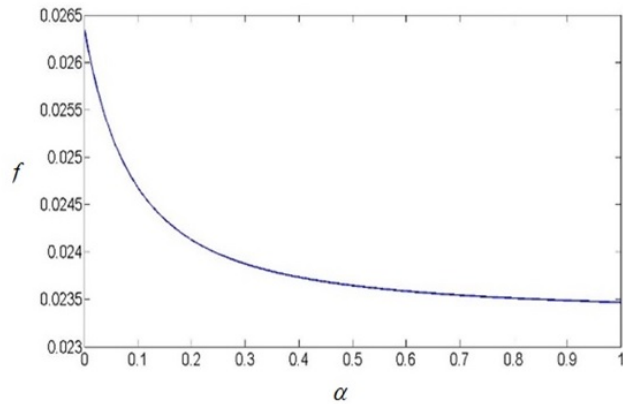


Figure 12. Plot of the frequency of the cnoidal waves versus α , having $\theta = 0.1$, $\vartheta = 0.1$, $V = 0.015$ and $\sigma_0 = -0.002$.

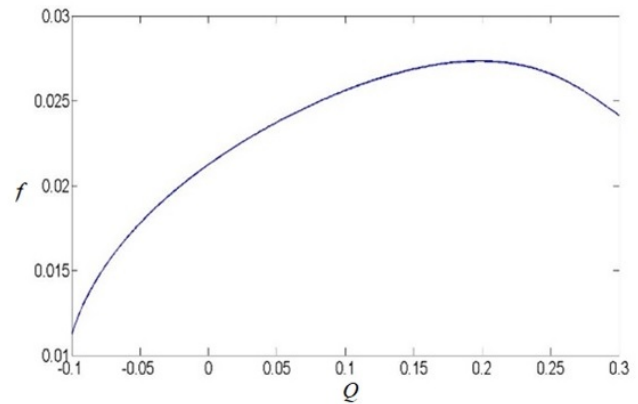


Figure 13. Plot of the frequency of the cnoidal waves versus Q , having $\theta = 0.1$, $\vartheta = 0.1$, $V = 0.015$ and $\sigma_0 = -0.002$.

it in previous articles and to avoid repetition, we refer you to them [28–31]. We consider the new variable as $\mu = \zeta - V_1 \tau$ where V_1 is the velocity of the nonlinear structure moving with the frame. With this variable change and by double integrating with respect to μ , we obtain the relation related to the law of conservation of energy as follows:

$$\frac{1}{2} \left(\frac{d\Psi}{d\mu} \right)^2 + v(\Psi) = 0 \tag{56}$$

Here Sagdeev potential $v(\Psi)$ is defined as

$$v(\Psi) = \frac{a}{6b} \Psi^3 - \frac{u}{2b} \Psi^2 + \sigma_0 \Psi - \frac{1}{2} \varepsilon_0^2 \tag{57}$$

In the above equation $V = V_1 - C_1$, σ_0 and ε_0 are integral constants. The periodic (cnoidal) wave solution of Eq 56 is as follows [29–32].

$$\Psi(\mu) = \beta_1 + (\beta_0 - \beta_1) cn^2(R\mu, l) \tag{58}$$

Here β_0 , β_1 and β_2 are the real roots of Sagdeev potential. Where cn is Jacobian elliptic function, whereas the parameters l , $0 < l < 1$ and R are defined as

$$l^2 = \frac{\beta_0 - \beta_1}{\beta_0 - \beta_2}, (0 < l < 1) \tag{59}$$

$$R = \left(\frac{a}{12b} (\beta_0 - \beta_2) \right)^{\frac{1}{2}} \tag{60}$$

4. Results and discussion

In this section, we investigate the combined effects of nonthermal and nonextensive parameters on the nature and properties of the ion acoustic wave in electron-positron-ion nonmagnetic plasma. Ion acoustic periodic (Cnoidal) waves may generate and propagate in the plasma medium only if Sagdeev potential

has three real roots. In order to have real roots, the following inequalities had to establish.

$$\left(O = \left(\frac{V}{a} \right)^2 - \sigma_0 \left(\frac{b}{a} \right) \right) > 0, \text{ and } 0 < \left[\frac{\beta_0 - \beta_1}{\beta_0 - \beta_2} \right] < 1$$

Acceptable values of α and Q for the formation of these ion acoustic periodic (Cnoidal) waves are obtained from these inequalities. In Figs 1 and 2 the Eqs O and l^2 are plotted in terms of Q for different α . These Figs show the range of acceptable values of Q . In these Figs, the allowable values of Q start from approximately -0.1 and with increasing α , the range of allowable values of Q increases. Fig 3 shows the set of allowable values α for different values Q . This Fig shows that for all the values defined for α we can have Cnoidal waves. Fig 4 shows the two-dimensional form of the allowable values Q and α , for which a periodic ion acoustic waves is formed. In the plot of these Figs σ_0 , V and θ are equal to -0.002, 0.015 and 0.1, respectively. In Fig 5 the nonlinear coefficient a is plotted versus two parameters Q and α . This Fig shows that the nonlinear coefficient a is positive for the allowable values of Q and which emphasizes the compression of the ion acoustic periodic waves. In Figs 6 and 7 the Sagdeev

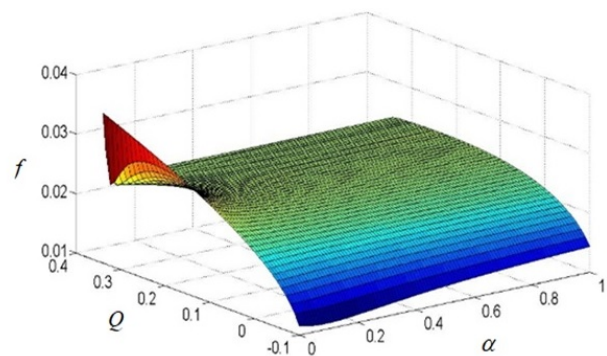


Figure 14. Plot of the frequency of the cnoidal waves versus Q , having $\theta = 0.1$, $\vartheta = 0.1$, $V = 0.015$ and $\sigma_0 = -0.002$.

potential $v(\Psi)$ is plotted versus Ψ for different values of Q and α respectively. Fig 6 shows that the width and depth of the potential well decreases with increasing Q to about 0.2 and then increases and Fig 7 shows that the Sagdeev potential becomes wider and deeper with increasing α potential. Figs 8 and 9 show the phase curve. The phase curve was plotted versus Ψ for different Q and α , respectively. The phase curve is repeated on the same path, and one complete cycle corresponds to one wavelength in the physical space. This implies that whenever the pseudo particle is velocity becomes zero, or in other words $d\Psi/d\mu = 0$ potential force reflects it back since $-dv(\Psi)/d\Psi$ does not vanish, and therefore, it oscillates between two points. [33]. Figs 10 and 11 show the effects of α and Q on the shape of the wave pattern, respectively. Fig 10 shows the wave pattern for Q of 0.1, 0.2 and 0.3 for $\alpha = 0.1$. This Fig shows that by increasing Q to $Q = 0.2$, the amplitude and wavelength of cnoidal waves decrease and then start to increase, and Fig 11 shows the wave pattern for $Q = 0.1$ for α of 0.1, 0.3 and 0.5. This Fig shows that with increasing α amplitude and wavelength of cnoidal wave's increase. Figs 12 and 13 show the frequency of the cnoidal waves versus α and Q , respectively. Fig 12 shows the frequency versus α for $Q = 0.1$. This figure shows that when f increases to about 0.5, the frequency decreases and then becomes almost constant. Fig 13 shows the frequency of the cnoidal waves versus Q for $\alpha = 0.1$. This Fig shows that with increasing Q , the frequency increases to about 0.2 and then the frequency decreases. Fig 14 shows the frequency of the cnoidal wave for the allowable values of two parameters α and Q . In Figs 12, 13 and 14, the quantities $V = 0.015$, $\sigma_0 = -0.002$, $\vartheta = 0.1$ and $\theta = 0.1$ is considered as constant values.

5. Conclusion

The study of this three-component plasma model with non-thermal and nonextensive distributed positrons and electrons shows that the cnoidal waves are not formed for all values related to nonextensivity (Q) and for each value α only a limited range of Q values is allowed to form cnoidal waves. As mentioned earlier, only values of α and Q are acceptable for which the Sagdeev potential has three real roots. Fig 4 shows the set of common values between all intervals. For these common values, the nonlinear coefficient of the KdV equation is positive, which indicates that the cnoidal waves in this interval are compressive. Examination of the diagrams shows that the effect of the parameter α on the width and depth of the potential well is greater than the parameter Q . The wavelength and amplitude of the cnoidal waves will increase more with increasing α compared to increasing the parameter Q . Examination of frequency diagrams shows that with increasing α , first the frequency decreases and then the trend of changes is almost constant. However, when the parameter Q increases, the frequency first increases and then decreases.

Conflict of interest statement:

The authors declare that they have no conflict of interest.

References

- [1] M. V. Goldman, M. M. Oppenheim, and D. L. Newman. *Nonlin. Proc. Geophys.*, **6**:221, 1999.
- [2] R. C. Davidson. *Methods in Nonlinear Plasma Theory*. Academic, New York, 1th edition, 1972.
- [3] R. Bostrom. *IEEE Trans. Plasma Sci.*, **20**:756, 1992.
- [4] P. O. Dovner, A. I. Eriksson, R. Bostrom, and B. Holback. *Geophys. Res. Lett.*, **21**:1827, 1994.
- [5] R. A. Cairns, A. A. Mamun, R. Bingham, R. Bastrom, R.O. Dendy, C.M. C. Narins, and P. K. Shukla. *Geophys. Res. Lett.*, **22**:2709, 1995.
- [6] C. Tsallis. *J. Stat, Phys.*, **52**:479, 1988.
- [7] P. Douglas, S. Bergamini, and F. Renzoni. *Phys. Rev. Lett.*, **96**:110601, 2006.
- [8] L. A. Gougam and M. Tribecher. *Astrophys. Space Sci.*, **331**:181, 2011.
- [9] H. R. Pakzad. *Astrophys. Space Sci.*, **334**:337, 2011.
- [10] M. Tribeche, L. Djebarni, and R. Amour. *Phys. Plasmas*, **17**:042114, 2010.
- [11] M. Tribeche, R. Amour, and P. K. Shukla. *Physical Review E*, **85**:037401, 2012.
- [12] R. Amour, M. Tribeche, and P. K. Shukla. *Astrophys Space Sci.*, **338**:287, 2012.
- [13] M. Farooq, A. Mushtaq, and M. Shamir. *Physics of Plasmas*, **25**:122110, 2018.
- [14] O. Bouzit, M. Tribeche, and A. S. Bains. *Physics of Plasmas*, **22**:084506, 2015.
- [15] M. Benzekka and M. Tribeche. *Physics of Plasmas*, **20**:083702, 2013.
- [16] W.F. El-Taibany, N.M. El-Siragy, E.E. Behery, A.A. El-Bendary, and R.M. Taha. *Chinese Journal of Physics*, **58**:151, 2018.
- [17] G. Williams, I. Kourakis, F. Verheest, and M. A. Hellberg. *Phys. Rev. E*, **88**:023103, 2013.
- [18] S. A. El-Tantawy, A. M. Wazwaz, and R. Schlickeiser. *Plasma Phys. Controlled Fusion*, **57**:125012, 2015.
- [19] A. Saha, N. Pal, T. Saha, M. K. Ghorui, and P. Chatterjee. *J. Theor. Appl. Phys.*, **10**:271, 2016.
- [20] S. Guo and L. Mei. *Phys. Plasmas*, **21**:082303, 2014.
- [21] S. Guo, L. Mei, and Z. Zhang. *Phys. Plasmas*, **22**:052306, 2015.
- [22] S. Rostampooran and S. Saviz. *J. Theor. Appl. Phys.*, **11**:127, 2017.
- [23] D. Dutta and B. Sahu. *Commun. Theor. Phys.*, **68**:117, 2017.

- [24] S. Ali Shan and H. Saleem. *AIP Adv.*, **7**:085119, 2017.
- [25] Y. Liu, Z. F. Shi, Y. Han, and B. Dai. *Phys. Plasmas*, **22**:032103, 2015.
- [26] R. Amour and M. Tribeche. *Phys. Plasmas*, **17**:063702, 2010.
- [27] H. Alinejad. *Astrophys Space Sci.*, **325**:209, 2010.
- [28] F. Farhadkiyaei and D. Dorrnian. *Contributions to Plasma Physics*, **58**:42, 2018.
- [29] E.F. El-Shamy. *Physical Review E.*, **91**:033105, 2015.
- [30] V.I. Karpman. *Nonlinear Waves in Dispersive Media*. Pergamon, Oxford, 1th edition, 1975.
- [31] F. Farhadkiyaei and D. Dorrnian. *Phys. Plasmas*, **24**:012107, 2017.
- [32] T. Kaladze, S. Mahmood, and H. Ur-Rehman. *Physica Scripta*, **86**:035506, 2012.
- [33] J. K. Chawla and M. K. Mishra. *Phys. Plasma*, **17**:102315, 2010.